Scientific Research Publishing

Open Journal of Geology, 2023, 13, 1271-1290
https://www.scirp.org/journal/ojg
ISSN Online: 2161-7589
ISSN Print: 2161-7570

Tracing the Origin of Metasedimentary Rocks in the Tortiya Diamond Region (Northern Côte d'Ivoire)

Tessia Miryam[1], Adingra Martial Pohn Koffi[1], Koffi Yao Augustin[1], Houssou Nestor[1], Allialy Marc Ephrem[1*], Kouassi Brice Roland[2]

[1]Félix Houphouët-Boigny University of Abidjan, Abidjan, Côte d'Ivoire
[2]Peleforo Gon Coulibaly University of Korhogo, Korhogo, Côte d'Ivoire
Email: *marcephremallialy7@gmail.com

How to cite this paper: Miryam, T., Koffi, A.M.P., Augustin, K.Y., Nestor, H., Ephrem, A.M. and Roland, K.B. (2023) Tracing the Origin of Metasedimentary Rocks in the Tortiya Diamond Region (Northern Côte d'Ivoire). *Open Journal of Geology*, **13**, 1271-1290.
https://doi.org/10.4236/ojg.2023.1312055

Received: November 7, 2023
Accepted: December 9, 2023
Published: December 12, 2023

Abstract

Metasedimentary rocks from the Tortiya diamondiferous region (northern Côte d'Ivoire), located in the Ivorian Paleoproterozoic domain, were analyzed with the aim of identifying their different petrographic facies, constraining their provenance and tectonic environment, and assessing the effects of sedimentary processes and weathering on the signature of their source rocks. These analyses were carried out with a view to helping trace the origin of Tortiya diamonds, which are generally hosted in these metasediments. Major and trace element geochemical data reveal that these samples are characterized by negative Eu anomaly values, low to moderate weathering index values and a high compositional variation index (ICV). These results led to the definition of these metasediments as immature sediments potentially originating from rapid erosion and sediment deposition from local sources. Chemical alteration index (CIA) values and Al_2O_3-(CaO^* + Na_2O)-K_2O composition space suggest low to medium degrees of meteoric alteration of the parent rock. These rocks therefore show poorly differentiated compositions from the parent rock and poor sediment sorting. Geochemical data and ratios of immobile elements, e.g. Al_2O_3/TiO_2, Cr/Th, Eu/Eu^* and (La/Yb)n, indicate that the clastic materials derive mainly from felsic to intermediate sources. Sedimentary tectonic discrimination diagrams demonstrate that most of the samples from the Tortiya diamond-bearing region were deposited on an active continental margin or in a continental arc-island environment. Although this region has a long history of diamond mining, its petrogenesis remains unresolved, and this petrogeochemical work is a step towards initiating scientific research in the area.

Keywords

Petrography, Geochemistry, Metasediments, Tortiya, Ivory Coast

1. Introduction

Paleoproterozoic domain that forms the northern and eastern parts of the Man-Léo Shield, which occupies the southern segment of the West African craton, consists of belts of metavolcanic and metasedimentary rocks intruded by different generations of granitoids, at the boundaries of which large tonalite batholiths, trondhjemites and granodiorites (TTG) [1] [2] are encountered. Geochronological studies on Birimian rocks suggest that they were formed between 2.3 and 2.0 billion (Ga) [1] [3] [4] [5]. They were deposited on deformed and metamorphosed basement rocks no older than 50 million (ma) [1]. They exposed Birimian age, accreted around 2.1 Ma during the Eburnean orogeny [3] [6] [7]. Tectonically, they were affected by medium-grade tectonometamorphism evolving from greenschist to amphibolite facies although granulite-facies rocks are also found in some very localized areas. Our study area lies in the north-western extension of the NNE-SSW-trending Ferkessédougou belt (northern Côte d'Ivoire). This furrow consists mainly of shales, sandstones and conglomerates affected by epizonal metamorphism.

Geochemical studies of the metavolcanic rocks of Birimian greenstone belts are numerous [1] [4] [5] [8] and varied, whereas Birimian sedimentary rocks in comparison have received very little attention [9] [10], despite representing a reliable source of information on the provenance and evolution of the Earth's crust [11]. While it is true that petrographic study, through the description of a rock's mineralogical assemblages, enables us to define part of its geological history, this step remains insufficient when it comes to examining metasediments. Geochemical examination, and more specifically rare earth element (REE) analysis, could be used effectively to assess the nature and evolution of the provenance of sedimentary history.

The main objective of this study is to determine the sources and tectonic setting of the metasedimentary rocks of the Tortiya diamond field. We focus on immobile elements such as rare earths and high field strength elements (HFSE) [5] as these elements are generally transferred quantitatively and unfractionated during sedimentary processes that may reflect the source rock signature [12] [13], unlike elements such as Si, Na, K, Ca, Mg, Rb and Sr [1] which are generally affected by even low-grade metamorphism or alteration.

2. Geological Settings

The study area is located in the Paleoproterozoic domain of Côte d'Ivoire (**Figure 1**) and consists mainly of ortho- and paraderivative magmatic and metamorphic rocks [14]. The magmatic rocks consist of granitoids and dioritoids.

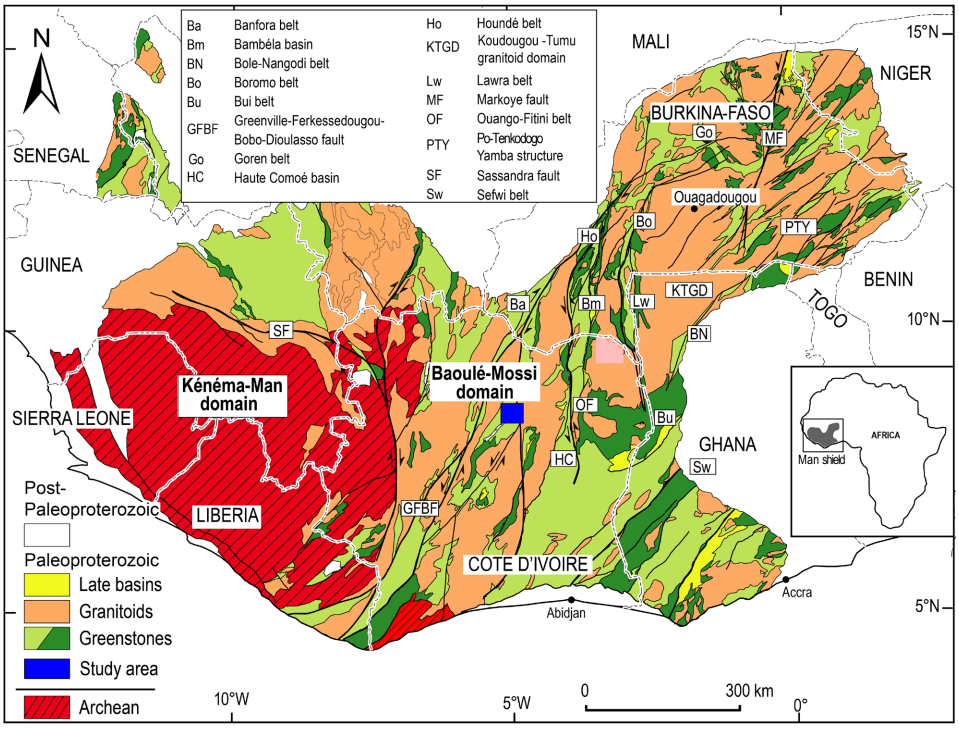

Figure 1. Simplified geological framework of the Man-Leo Dorsal (modified from BRGM's SIGAfrique map).

Granitoids are essentially non-oriented biotite bearing granites and biotite-hornblende metagranodiorites with a general NNE-SSW direction. Dioritoids consist mainly of gabbros. Metamorphic rocks include schists, metagabbros, metadolerites, amphibolo-pyroxenites and biotite and/or hornblende bearing metagranodiorites. Schists form a diverse direction N22˚ band across our study area, consisting of alternating greywacke schists and arkosic schists. These latter are crosscutted by with lenses of conglomeratic schist [15] (**Figure 2**). The tectonics are represented by global trending ESE-WNW faults and strike-slip that generally affect the shales.

3. Sample Description

Four samples (sample TOR 04, sample TOR 50, sample TOR 78, sample TOR C) collected in the field were subjected to geochemical analysis. To the naked eye, they are mainly characterized by a distinctive dark-gray color, considerable hardness, and massive structure (**Figure 3**). They consist of subangular to subrounded, moderately to poorly sorted grains. On the microscopic scale, the mineralogy of greywacke consists of quartz (20% - 35%) sometimes showing rolling extinction, alkali feldspars (15% - 25%) presented in dusty-looking clasts, lithic clasts (20% - 25%), sericite-included plagioclase (approx. 15%) and a small amount of sericite and a few chlorite-altered biotites (<5%). Interpenetration of the edges of the quartz grains is certainly due to compaction and distribution of phyllite minerals (muscovite) around certain quartz and feldspar clasts mark a clear schistosity. Two samples (TOR 61 and TOR 17) are meta-arenites with a whitish

color at outcrop. Microscopically, they are composed of quartz with a mosaic structure and large rolling extinction crystals representing around 75% of the rock. Muscovites show a preferential orientation and occupy the interstices like a filling. Feldspars account for around 15% of the rock. The rock has undergone slight stretching and alignment of quartz and feldspars.

4. Methodology

Six (06) rock samples were selected and sent to the Bureau Veritas Côte d'Ivoire mineral analysis laboratory to determine their major and trace element compositions by atomic emission spectrometry (ICP-AES) and mass spectrometry (ICP-MS).

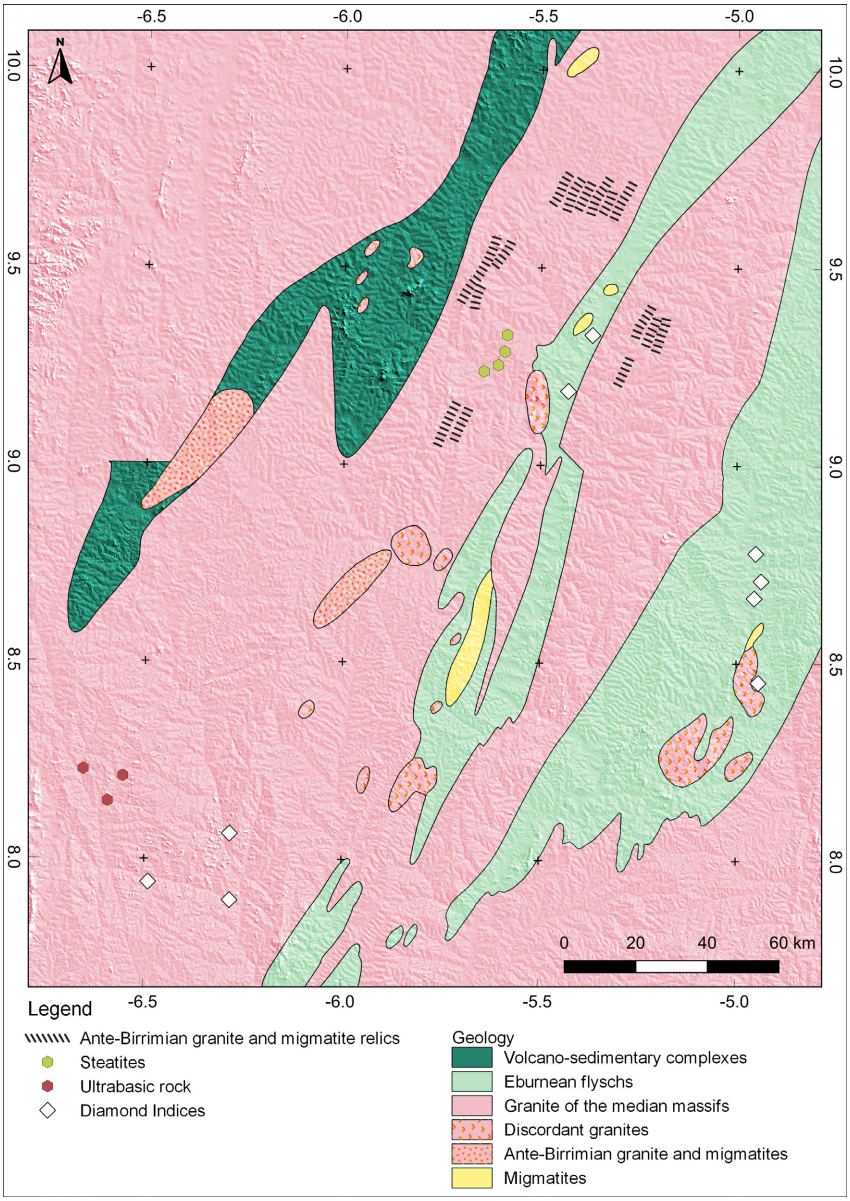

Figure 2. Simplified geological map of the Tortiya diamond deposit (modified after Bardet, 1974).

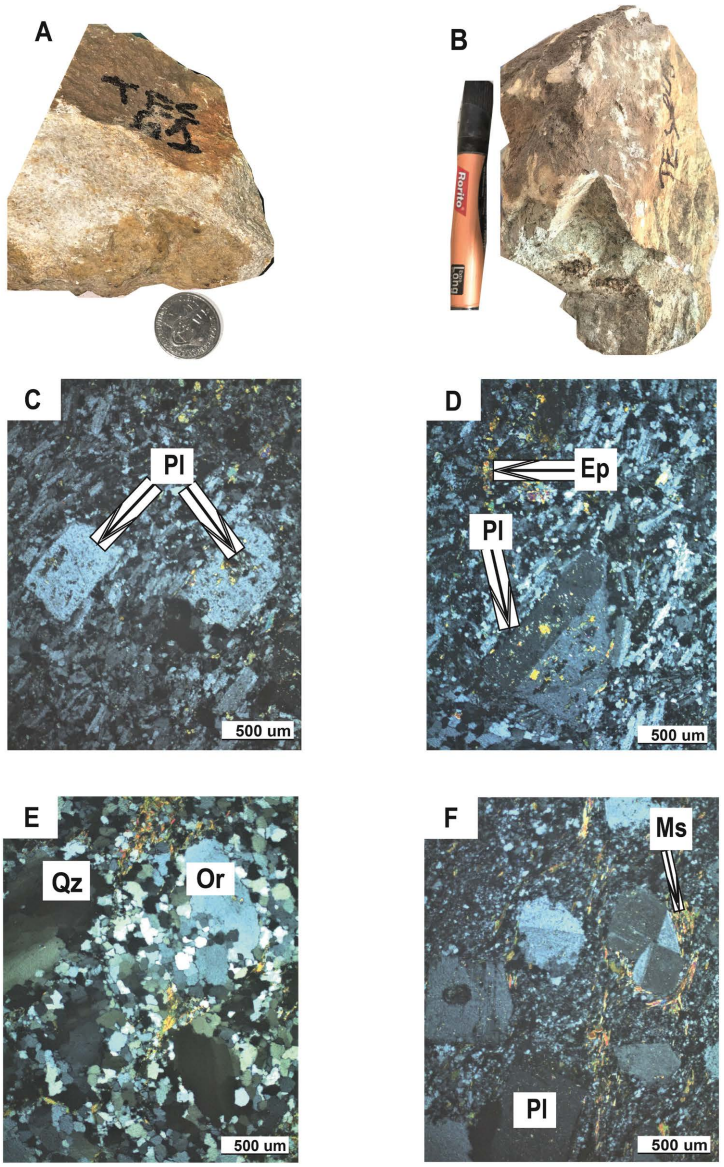

Figure 3. (A), (B): macroscopic sample of arenite and greywacke from Tortiya; (C), (D): thin section of greywacke showing altered plagioclase; (E), (F): section of arenite showing rolling quartz and interpenetrating edges; (F: muscovite molded around feldspar.

The samples were successively jaw crushed and then roller crushed. The powders are divided by quartering using an equiproportional separator. Their particle size is reduced to 70 - 80 µm. Chemical analyses are carried out on 10 grams of rock powder and fifty-six chemical elements are assayed.

These are:

- Major elements (12): SiO_2, Al_2O_3, Fe_2O_3, CaO, MgO, Na_2O, K_2O, TiO_2, MnO, P_2O_5, Cr_2O_3 and loss on ignition (LOI). 11 elements were analyzed by atomic emission spectrometry (ICP AES), while Cr_2O_3 was quantified by mass spectrometry (ICP MS);

- Base metals (8): Ag, Co, Cu, Mo, Ni, Pb, Zn and Cd obtained by an etching

(AQ 200). This procedure is followed by atomic emission spectrometry emission spectrometry (ICP AES) for determining the content;

- Volatile elements (6): As, Bi, Hg, Sb, Se and Be were first digested by Aqua Regia (AQ 200) and then quantified by plasma torch mass spectrometry mass spectrometry (ICP-MS);

- Trace elements and rare earth elements REE (30 elements): Ba, Ce, Cs, Dy, Er, Eu, Ga, Gd, Hf, Ho, La, Lu, Nb, Nd, Pr, Rb, Sm, Sn, Sr, Ta, Tb, Th, Tl, Tm, U, V, W, Y, Yb and Zr first undergo lithium-boron melting before dissolving dissolution. Finally, plasma torch mass spectrometry (ICP MS) was used to quantify them.

5. Results

5.1. Major Elements

Samples analyzed showed high SiO_2 contents ranging from 67.11% to 94.97%. TiO_2 compositions ranged from 0.04 to 0.66 and MgO from 0.08% to 2.27%. CaO and Al_2O_3 contents range from 0.02% - 3.62% and 2.34% - 13.81% respectively, and Fe_2O_3 contents from 1.06% to 6.13%. SiO_2/Al_2O_3 ratios ranged from 4.24 to 40.58 and Na_2O/K_2O ratios from 0.01 to 11.33 (**Table 1**). As a result, most of samples fall into greywackes field and 2 samples fall into sub-arenites field in diagram Log (Na_2O/K_2O) vs Log (SiO_2/Al_2O_3) by [16] (**Figure 4**). Diagram Log (SiO_2/Al_2O_3) vs Log (Fe_2O_3/K_2O) by [17] (**Figure 5**) presents most samples as wackes except for 2 samples described as sublitharenites as does diagram Al_2O_3/ $CaO + Na_2O + K_2O$ by [18] except for TOR 61 identified as a sub-arkose by this diagram. However, diagram (**Figure 6**) by [19] specifies that these samples are all sedimentary origin.

5.2. Trace-Element

Composition of large-ion lithophile elements (LILE) such as Rb (14 - 63.3 ppm), Sr (65.3 - 796.6 ppm) and Ba (90 - 533 ppm) shows varying degrees of variation. The average Sr content (381.6) far exceeds that of the Post-Archean Australian Shale (PAAS), which is 200 ppm according to [12] [20] and the Upper Continental Crust (UCC), which is 320 ppm according to [21] and considered as references. Average Ba concentration (357.7) is much lower than that of the PAAS (650 ppm) and the UCC (628 ppm). The HFSE content such as Nb (0.4 - 7.2; average grade: 4.4); Ta (0.1 - 0.4; average grade: 0.31) and Hf (1 - 4.4; average grade: 3.4) varies little and their average grades are roughly like those of PAAS and UCC (**Table 1**).

Average Zr content (35.5 - 170, average grade: 125.9) is much lower than that of PAAS (210 ppm) and UCC (193 ppm). Transition elements such as Co (0.6 - 15.8; mean grade: 9.6), Ni (0.9 - 32.6; mean grade: 21.6) and V (18 - 87; mean grade: 58.7) show wide variations, and mean grades are lower than those reported by PAAS and UCC (**Table 1**).

Table 1. Major elements (wt%) and trace elements (ppm) of the metasedimentary rocks from the Tortiya Formation in comparison to other sediments from references.

Samples	Grauwacke				Arenite		PAAS	UCC
	TOR 04	CONG-SAINT	TOR 50	TOR 78	TOR 17	TOR 61		
Major elements (%Wt)								
SiO_2	71.54	70.96	71.72	67.11	87.66	94.97	62.80	66.60
Al_2O_3	13.81	13.67	14.26	15.82	5.55	2.34	18.9	15.40
Fe_2O_3	4.18	5.16	4.82	6.13	2.88	1.06	6.50	5.04
MnO	0.09	0.1	0.08	0.07	0.04	0.02	0.10	0.11
MgO	1.09	1.67	1.27	2.27	0.19	0.08	2.20	2.48
CaO	3.62	2.48	3.59	1.31	0.46	0.02	1.30	9.59
Na_2O	4.42	3.67	3.76	3.17	1.52	0.01	1.20	3.27
K_2O	0.39	1.37	0.49	2.11	1.52	0.7	3.70	2.80
TiO_2	0.46	0.56	0.58	0.66	0.23	0.04	1.00	0.64
P_2O_5	0.09	0.14	0.13	0.15	0.04	0.04	0.16	0.15
PF	0.64	0.9	0.49	1.66	−0.13	0.26		
Total	100.33	100.68	101.19	100.46	99.96	99.54		
Na_2O/K_2O	11.33	2.68	7.67	1.50	1.00	0.01	3.08	0.86
K_2O/Na_2O	0.09	0.37	0.13	0.67	1.00	70.00	3.08	0.85
SiO_2/Al_2O_3	5.18	5.19	5.03	4.24	15.79	40.59	3.32	4.32
Al_2O_3/TiO_2	30.02	24.41	24.59	23.97	24.13	58.50	18.90	24.06
CIA	42.03	55.47	50.84	64.03	57.56	75.54		
ICV	1.32	1.10	1.02	0.99	1.23	0.82		
PIA	38.77	56.23	50.88	67.20	61.41	100.00		
Trace (ppm)								
As	1.1	0.9	0.5	0.5	0.7	0.5		
Ba	90	533	95	507	387	530	650	628
Be	1	1	1	2	2	1		
Bi	0.1	0.1	0.1	0.1	0.1	0.1		
Cd	0.1	0.1	0.1	0.1	0.1	0.1		
Ce	44.6	65.1	53.2	48.3	29.9	46.3	79.6	63.0
Co	9.6	15.8	12.1	15.8	4.2	0.6		
Cs	0.5	1.3	1.4	1.2	1.2	0.3	15	4.9
Cu	11.9	26.3	12.2	33.4	2.3	3.8		28
Dy	2.38	3.3	2.62	2.41	1.45	3.1	4.48	3.90
Er	1.27	2.03	1.36	1.71	0.81	0.71	2.85	2.30
Eu	1	1.29	1.16	1.03	0.6	1.82	1.08	1.00
Ga	9.9	15.4	11.3	14.2	3.7	0.5		17.5
Gd	2.87	4.23	3.13	3.15	2.11	5.38	4.66	4.00
Hf	4.3	4.4	3.7	3.9	3.1	1	5.00	5.30

Continued

Ho	0.45	0.69	0.49	0.47	0.31	0.37	0.99	0.83
La	26.4	34.3	26	22.3	17.7	37.1	38.0	31.0
Lu	0.18	0.29	0.2	0.24	0.14	0.05	0.43	0.31
Mo	0.2	0.1	0.3	0.2	0.4	0.5		
Nb	5.3	7.2	5.2	5.9	2.8	0.4	19.0	12.0
Nd	22.6	27.9	23.1	22.5	16	36	33.9	27.0
Ni	23.8	32.6	31.7	31.3	10.6	0.9	55.0	47.0
Pb	3.6	2.7	1.8	1.9	2.9	1.7	20.0	17.0
Pr	5.72	7.54	5.91	5.85	4.07	8.63	8.83	7.10
Rb	14	63.3	27.5	66.5	34.6	14.7	160	82
Sb	0.1	0.1	0.1	0.1	0.1	0.1		
Sm	3.73	5.08	4.01	4.08	2.69	6.77	5.55	4.70
Sn	1	1	1	1	1	1		
Sr	796.6	470.3	543.5	288.6	125.4	65.3	200	320
Ta	0.4	0.4	0.4	0.4	0.2	0.1	1.28	0.90
Tb	0.38	0.6	0.44	0.43	0.27	0.66	0.77	0.70
Th	7	6.7	4.8	5.3	3.7	1.2	14.6	10.5
Tm	0.18	0.28	0.2	0.22	0.12	0.07	0.41	0.30
U	1.4	1.2	0.9	1.5	0.8	0.3	3.10	2.70
V	51	87	69	84	42	18	150	97.0
W	0.5	0.7	0.6	1.5	0.6	0.5		
Y	12.1	19.4	12.4	13.4	8.2	6.9	27.0	35.0
Yb	1.18	1.95	1.43	1.57	0.85	0.4	2.82	2.00
Zn	42	51	42	68	14	1		67.0
Zr	160.4	170	135.8	137.7	116.4	35.5	210	193
Eu/Eu*	0.93	0.85	1.00	0.88	0.77	0.92	0.66	0.72
(La/Yb)N	15.08	11.86	12.26	9.58	14.04	62.53	9.20	10.53
(La/Sm)N	4.45	4.25	4.08	3.44	4.14	3.45	4.30	4.12
ΣREE	112.94	154.58	123.25	114.26	77.02	147.36	184.4	148.1

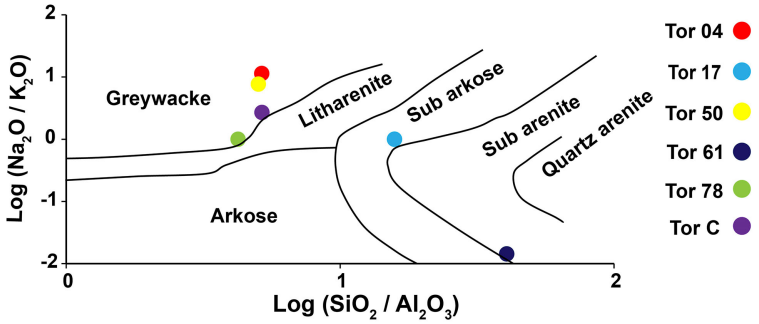

Figure 4. Geochemical classification of metasediments from the studied areas (Modified from Pettijohn *et al.*, 1972).

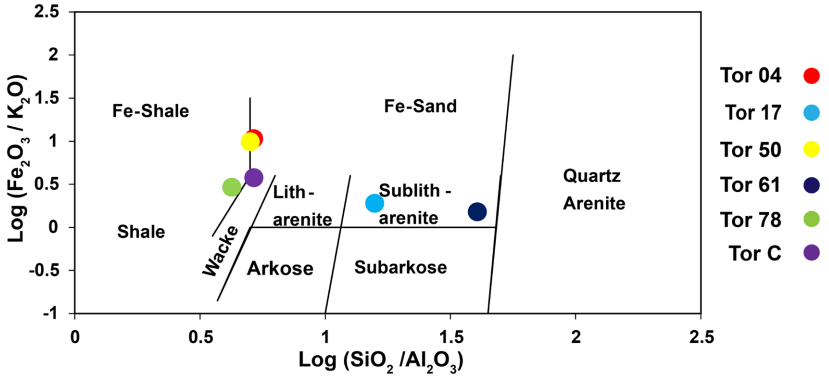

Figure 5. Geochemical classification of sediments from the studied area (After Herron, 1988).

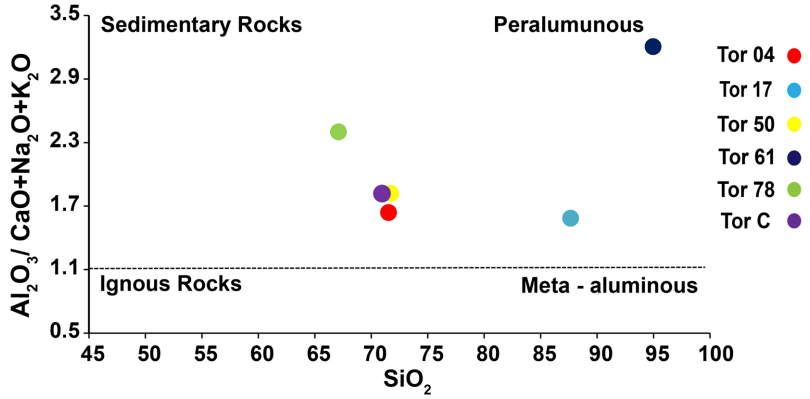

Figure 6. Discrimination diagram by Chappell and White (1974; 1977) applied to Tortiya's metasediments.

6. Discussion

6.1. Element Mobility

Tortiya metasedimentary samples have not undergone significant secondary alteration, as evidenced by their low loss on ignition (LOI), ranging from −0.13 to 1.66 (all samples have LOI values below 2). As they have undergone low metamorphism, mobility of major and trace elements and on isotopic compositions needs to be assessed.

6.2. Alteration of Metasediments

Alteration in source zones can lead to relative depletion of alkaline elements and LILEs and enrichment in TiO_2 and Al_2O_3 in clastic sedimentary rocks [22] [23]. Chemical Index of Alteration (CIA) [24], the Plagioclase Alteration Index (PIA) [25] and Compositional Variation Index (ICV) [26] can be used to quantitatively assess the degree of rock alteration (**Table 1**). CIA index measures the extent to which feldspars have been transformed into Ca-, Na- and K-depleted aluminous clays relative to the unweathered source and is defined as follows:

$$CIA = [Al_2O_3/(Al_2O_3 + CaO^* + Na_2O + K_2O)] \times 100 \text{ (molar proportions)},$$

where CaO* represents the CaO content of the silicate fraction.

On a scale of 40 to 100, unweathered igneous rocks have CIA values of 45 to 55, while moderately weathered shales have CIA values of 70 to 75. Intense alteration of the feldspars in a rock result in high concentrations of residual clays (kaolinite and/or gibbsite) and produces CIA values close to 100.

CIA values for metasediments in the Tortiya area range from 42.03 to 75.53 with an average value of 57.57 higher than those for fresh UCC [17] [21] but lower than those for PAAS (70 - 75) [22], implying a low to moderate degree of alteration of the source rocks (**Figure 6**). The low CIA values and negative Eu anomalies (for TOR 61 and TOR 17 arenites) are properties of juvenile crustal material from local sources and suggest high erosion rates, low transport, poor sorting, and rapid sediment deposition [27] [28].

PIA (PIA = $[Al_2O_3\ K_2O]/[Al_2O_3 + CaO^* + Na_2O - K_2O] \times 100$) is like the CIA but is not influenced by K redistribution and is commonly used to describe plagioclase alteration [25]. For fresh rocks, the PIA is 50, while for clay minerals such as kaolinite, illite and smectite, PIA is around 100 [25]. PIA values for metasedimentary rocks in the Tortiya area range from 60 to 83 and have an average value of 71, and these values suggest that the source of the metasedimentary rocks had a relatively low to moderate degree of alteration. Furthermore, the high CIA content of TOR 61 suggests that this sample is geochemically and texturally mature.

ICV (ICV = $[Fe_2O_3 + K_2O + Na_2O + CaO + MgO + TiO_2]/Al_2O_3$) was proposed by [26] [29] and represents another important chemical index for measuring the abundance of alumina relative to other major cations, indicating the compositional maturity of a rock. Non-clay minerals have higher ICV values than clay minerals; consequently, ICV values decrease with increasing degree of alteration and/or rock maturity. ICV values for metasedimentary rocks in the Tortiya formation range from 0.82 to 1.32, with an average value of 1.08, suggesting moderate weathering and/or maturity of the source.

6.3. Origin

Since the source of the metasedimentary rocks studied are not highly altered (CIA < 80) and they are chemically immature ($SiO_2/Al_2O_3 < 6$). Apart from the TOR 17 and TOR 61 arenites, the geochemical composition of the metasedimentary rocks studied may better reflect the properties and characteristics of the provenance.

6.3.1. Evidences of Major Elements

Previous researchers have asserted that the Al_2O_3/TiO_2 ratio is one of the most functional provenance indicators for sedimentary rocks [30] [31]. Al_2O_3/TiO_2 ratios of sandstones are basically identical to those of their source rocks [32]. Consequently, the Al_2O_3/TiO_2 ratio represents a good indicator of source rocks, particularly for igneous source rocks. [33] reported that sediments from mafic rocks show $Al_2O_3/TiO_2 < 14$ ratios and sediments from felsic rocks show $Al_2O_3/$

TiO_2 ratios between 19 and 28. Al_2O_3/TiO_2 ratios of the metasedimentary rocks of the Tortiya Formation range from 23.96 to 58.5 (mean = 30.96) (**Table 1**), indicating that the source materials are mainly from felsic to intermediate igneous sources.

Alteration trend of Tortiya samples in the Al_2O_3-($CaO^* + Na_2O$)-K_2O (A-CN-K) diagram [34] is broadly parallel to the A-CN line, suggesting K_2O loss and plagioclase abundance in the grauwacke's mineralogical composition TOR 04, 50, define their source rock as a gabbro. The intersection of the alteration trend with the feldspar line establishes the source rock of greywacke TOR C as a basalt and that of grauwacke TOR 78 as an andesite. Finally, according to the diagram, the TOR 17 and 61 arenites are derived from granite (**Figure 7**). According to the plot of Tortiya samples on the discriminant diagram of [18], the sediments studied derived from mafic igneous sources and intermediate provenance. Grauwackes TOR 04, 50 and TOR C have an intermediate provenance, while TOR 78 has a mafic provenance and arenites TOR 17 and 61 have a sedimentary provenance (**Figure 8**).

6.3.2. Trace Element Evidences

Multi-element diagrams normalized to the upper crust according to the values of [12] (**Figure 9**) show quite different profiles, grouped together by similarity of appearance. The multi-element spectra of TOR 61 and TOR 17 arenites show positive anomalies in Ba, K, Ta, La and Nd and negative anomalies in Nb, Sr and P. TOR 61 also shows negative anomalies in Ti and Sr and positive anomalies in Sm and Y. TOR C and 78 show negative anomalies in Nb, Zr, Tb and Th and positive anomalies in Ta, Ba, K, Ce, Nd and Sm. Finally, grauwackes 04 and 50 show negative anomalies in Ta, Ba, K, Ce and P and positive anomalies in Nb, Th, Sr and Ti. REEs are insoluble trace elements with very low mobility during lower-gradient metamorphism, weathering, hydrothermal alteration, and diagenesis [20]. As a result, they are reliable in determining the provenance of metasedimentary rocks. In general, volcanic-mafic rocks range from light rare-earth depletion (tholeiitic) to heavy rare-earth enrichment (calc-alkaline), while felsic rocks show light rare-earth enrichment. The sum of rare earth contents (∑REE) in Tortiya metasediments ranges from 77.02 to 154.58 ppm (**Table 1**). **Figure 10** shows that the spectra of TOR samples C, 04, 50, 17 and 78 evolve in a similar way and present identical parallel alleles in them with an enrichment in light rare earths (LREE) such as La, Ce, Pr, Nd, Pm, Sm, Eu and Gd. Beyond gadolinium, heavy rare earths (Tb, Dy, Ho, Er, Tm, Yb, Lu) show a slight concavity (TOR 17), sometimes spreading out into flat profiles (TOR C, 04, 78). However, the TOR 61 spectrum is depleted in heavy rare earths. Chondrite-normalized La to Yb ratios (La/Yb)N range from 9.58 to 62.53 (**Table 1**) for the metasediment samples. The TOR 61 arenite has the highest (La/Yb)N ratio. Its spectrum shows a well-marked negative Ce anomaly. Grauwackes samples TOR 04 and TOR 78 show a slight negative Europium (Eu) anomaly, with Eu/Eu^* ratios ranging from 0.77 to 1.00 (**Table 1**) and an average of 0.88 close to UCC ($Eu/Eu^* = 0.72$). Ex-

cept for the arenite TOR 61, all other samples are exempt from Ce anomalies. Furthermore, the rocks studied show intense fractionation between light and heavy rare earths, indicating that mafic igneous rocks are not a significant source.

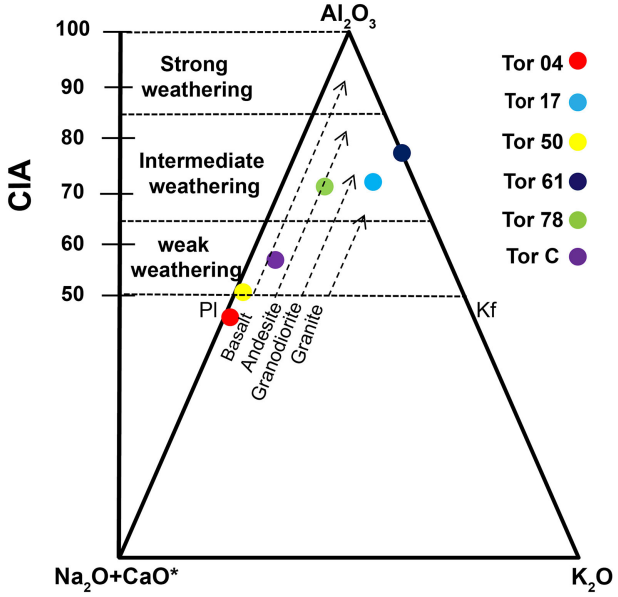

Figure 7. A-CN-K ternary diagram showing weathering trends of the Tortiya's metasediments. (Modified from Nesbitt and Young, 1982); CIA values can range from 50 for fresh primary igneous rocks to a maximum of 100 for the most weathered rocks (Fedo *et al.*, 1995).

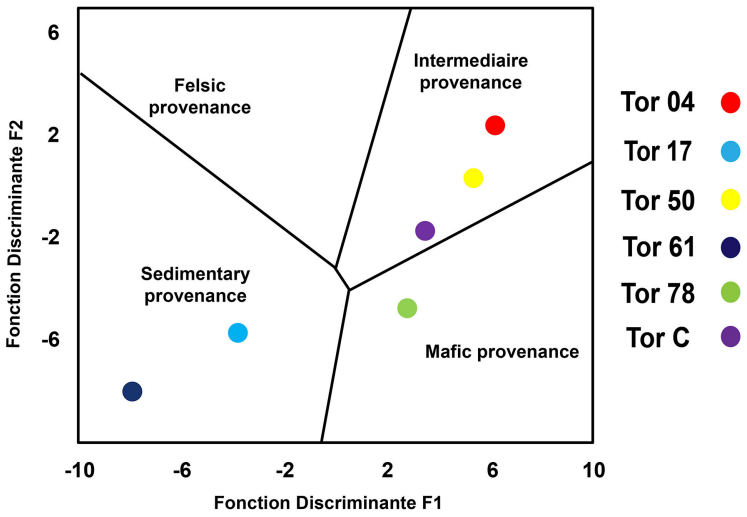

Figure 8. Discrimination diagrams for the provenance signature of sedimentary rocks of Tortiya Formation using major elements (after Roser and Korsch 1988).

Discriminiant Function (DF1) = $-1.773TiO_2 + 0.607Al_2O_3 + 0.76\ Fe_2O_3(T) - 1.5MgO + 0.616CaO + 0.509Na_2O - 1.224K_2O - 9.09$

Discriminiant Function (DF2) = $0.445TiO_2 + 0.07Al_2O_3 - 0.25\ Fe_2O_3(T) - 1.42\ MgO + 0.438CaO + 1.475\ Na_2O + 1.426K_2O - 6.861$

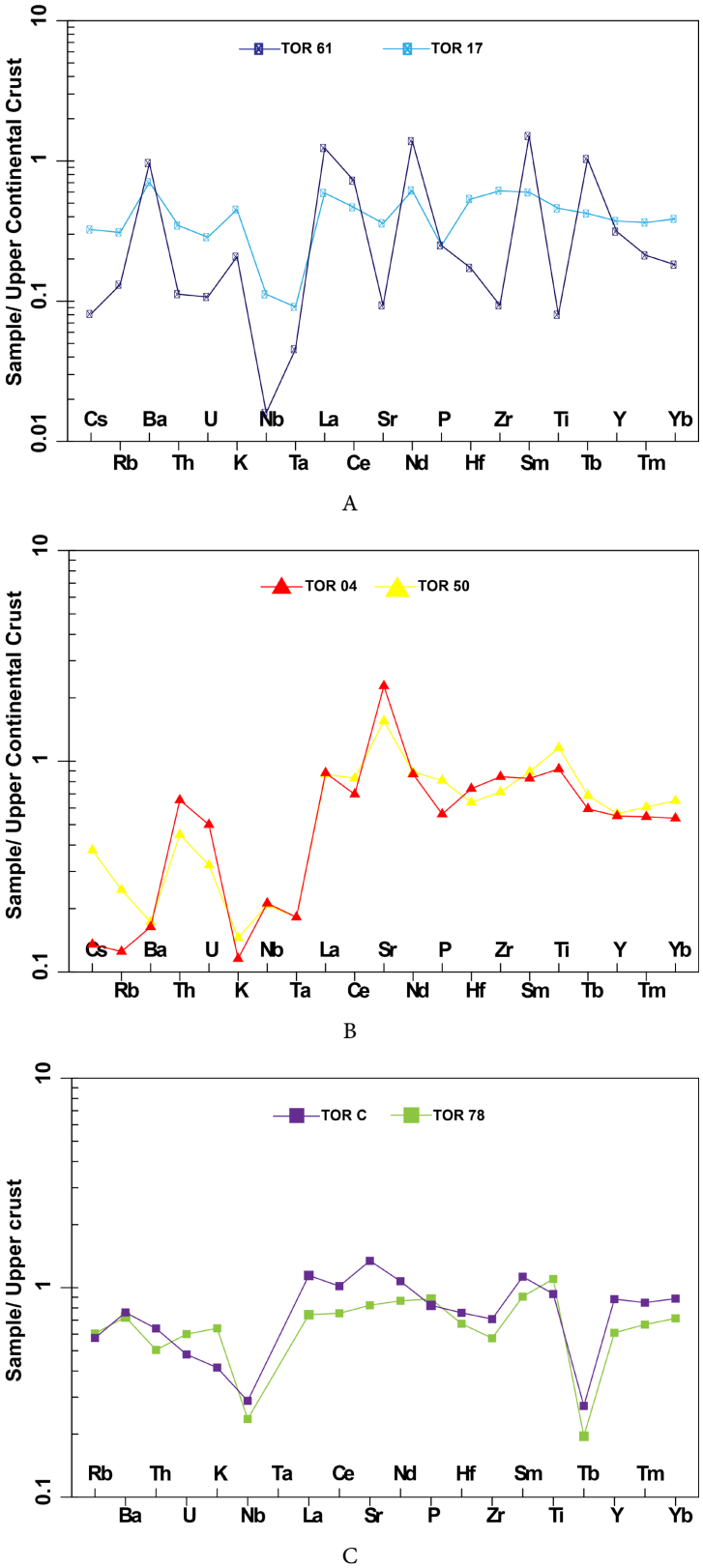

Figure 9. Spider diagrams of metasedimentary rocks from Tortiya diamond field. (A) et (B) normalized to the upper continental crust; (C): normalized to the upper crust. Normalization values after Sun and McDonough (1989).

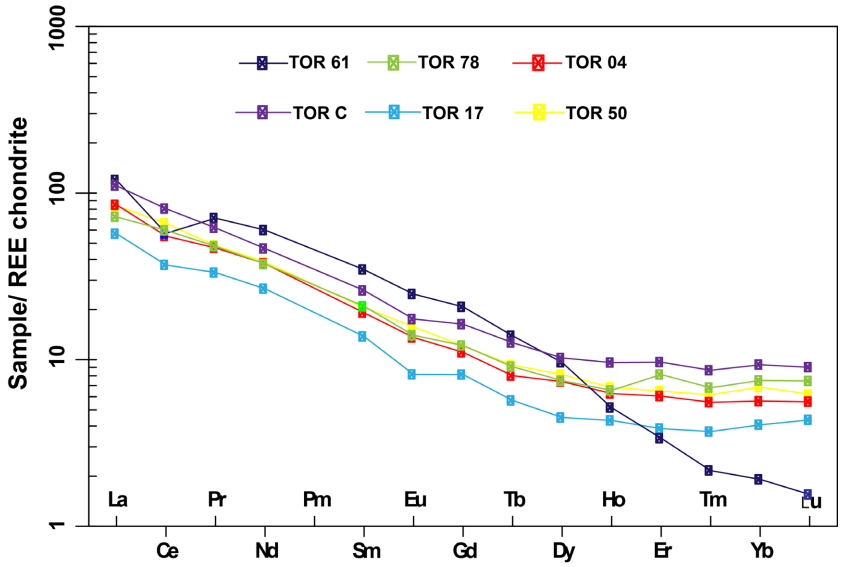

Figure 10. Chondrite normalized REE patterns of metasediments rocks from Tortiya. Normalization values after Boyton (1984).

Transition elements (Cr, Sc, Ni, Co and V) are preferentially concentrated in mafic minerals such as pyroxenes and olivines. This is why sedimentary rocks derived from their erosion are characterized by high concentrations of these elements [35]. The Tortiya metasediments show only low levels of these compatible elements (**Table 1**), which therefore rules out the exposure of significant mafic rocks in origin of these metasediments. Also, as shown in **Figure 11** by [36] illustrating Rb vs. K2O diagram discriminating sedimentary rock provenance, the metasediments studied fall within the intermediate to acidic rock field once again.

6.4. Tectonic Setting

It has been shown that the geochemical compositions of sediments can be linked to plate tectonic processes, making geochemistry a powerful tool for the recognition of ancient tectonic settings [11] [12] [18] [37]-[42]. Some major element discrimination diagrams (K_2O/Na_2O versus SiO_2 and SiO_2/Al_2O_3 versus K_2O/Na_2O) (**Figure 12**) have been used to distinguish different tectonic settings [18] [41].

In these two (2) diagrams, samples TOR C, 50 and 78 are in the oceanic island-arc margin field, while sample TOR 04 is in the active continental margin field and sample TOR 61 in the passive margin field. In addition, samples TOR C, 17 and 78 exhibit evolved arc properties with felsic plutonic detritus, while sample TOR 50 displays arc tectonic properties with basaltic and andesitic detritus. Geochemical studies carried out on metasediments from the SASCA domain [43] in southwestern Côte d'Ivoire and the southeastern Comoé basin [44] suggest that they also belong to the oceanic island arc and active continental margin domains.

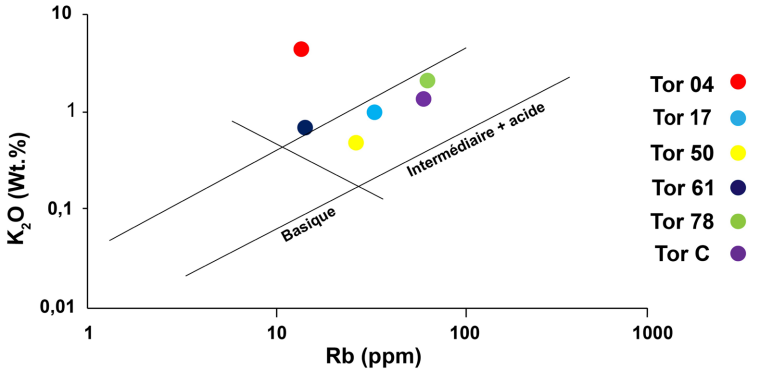

Figure 11. K_2O-Rb diagram showing variation of source composition for the metasedimentary rocks from Tortiya by Shaw (1968).

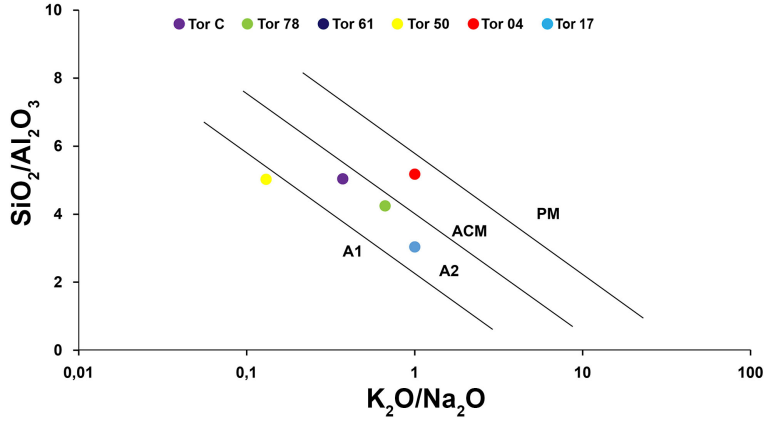

A

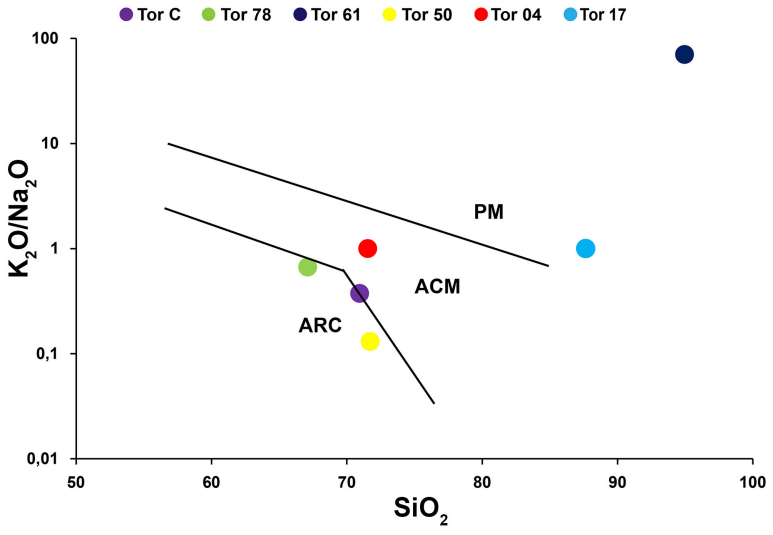

B

Figure 12. Tectonic discrimination diagrams for sedimentary rocks, (A) after Maynard *et al.* (1982) and (B) after Roser and Korsch (1986). ARC, oceanic island-arc margin; ACM, active continental margin; PM, passive margin; A1, arc setting, basaltic and andesitic detritus; A2 = evolved arc setting, felsic plutonic detritus.

7. Conclusions

The low CIA PIA and ICV values and negative Eu anomalies suggest that these metasediments are derived from locally sourced juvenile crustal material that has undergone poor weathering, erosion, transport and rapid sediment deposition.

Based on geochemical analyses of metasediments from Tortiya area, the following conclusions have been drawn:

1) Tortiya metasediment samples identified as wackes and sub-arkoses probably originate from felsic to intermediate (granite-andesite) sources.

2) They would have been emplaced in a geodynamic environment of active to passive continental margin and/or evolved island-arc ocean margin.

To complete this analysis, we suggest electron microprobe analyses of the heavy minerals in the sediments, in order to search for any link with ultrabasics. It would also be advisable to combine these results with geophysical and structural analyses to elucidate the origins of the diamonds contained in the Tortiya metasediments.

Acknowledgements

We would like to thank the management and staff of the exploration department of the "Société pour le Développement des Mines en Côte d'Ivoire" for their technical support and the accessibility of their property for field work. This research was funded by the Agate project and the UEMOA excellence grant.

Conflicts of Interest

The authors declare no conflicts of interest regarding the publication of this paper.

References

[1] Abouchami, W., Boher, M., Michard, A. and Albarede, F. (1990) A Major 2.1 Ga Event of Mafic Magmatism in West Africa: An Early Stage of Crustal Accretion. *Journal of Geophysical Research*: *Solid Earth*, **95**, 17605-17629. https://doi.org/10.1029/JB095iB11p17605

[2] Dampare, S.B., Shibata, T., Asiedu, D.K., Osae, S. and Banoeng-Yakubo, B. (2008) Geochemistry of Paleoproterozoic Metavolcanic Rocks from the Southern Ashanti Volcanic Belt, Ghana: Petrogenetic and Tectonic Setting Implications. *Precambrian Research*, **162**, 403-423. https://www.sciencedirect.com/science/article/pii/S0301926807002823 https://doi.org/10.1016/j.precamres.2007.10.001

[3] Hirdes, W. and Davis, D.W. (1998) First U Pb Zircon Age of Extrusive Volcanism in the Birimian Supergroup of Ghana/West Africa. *Journal of African Earth Sciences*, **27**, 291-294. https://doi.org/10.1016/S0899-5362(98)00062-1 https://www.sciencedirect.com/science/article/pii/S0899536298000621

[4] Béziat, D., Dubois, M., Debat, P., Nikiéma, S., Salvi, S. and Tollon, F. (2008) Gold Metallogeny in the Birimian Craton of Burkina Faso (West Africa). *Journal of African Earth Sciences*, **50**, 215-233. https://www.sciencedirect.com/science/article/pii/S1464343X07001744

https://doi.org/10.1016/j.jafrearsci.2007.09.017

[5] Sylvester, P.J. and Attoh, K. (1992) Lithostratigraphy and Composition of 2.1 Ga Greenstone Belts of the West African Craton and Their Bearing on Crustal Evolution and the Archean-Proterozoic Boundary. *The Journal of Geology*, **100**, 377-393. https://doi.org/10.1086/629593

[6] Liégeois, J.P., Claessens, W., Camara, D. and Klerkx, J. (1991) Short-Lived Eburnian Orogeny in Southern Mali. Geology, Tectonics, U-Pb and Rb-Sr Geochronology. *Precambrian Research*, **50**, 111-136. https://doi.org/10.1016/0301-9268(91)90050-K https://www.sciencedirect.com/science/article/pii/030192689190050K

[7] Boher, M., Abouchami, W., Michard, A., Albarede, F. and Arndt, N.T. (1992) Crustal Growth in West Africa at 2.1 Ga. *Journal of Geophysical Research*: *Solid Earth*, **97**, 345-369. https://doi.org/10.1029/91JB01640

[8] Leube, A., Hirdes, W., Mauer, R. and Kesse, G.O. (1990) The Early Proterozoic Birimian Supergroup of Ghana and Some Aspects of Its Associated Gold Mineralization. *Precambrian Research*, **46**, 139-165. https://www.sciencedirect.com/science/article/pii/0301926890900707 https://doi.org/10.1016/0301-9268(90)90070-7

[9] Anani, C.Y., Bonsu, S., Kwayisi, D. and Asiedu, D.K. (2019) Geochemistry and Provenance of Neoproterozoic Metasedimentary Rocks from the Togo Structural Unit, Southeastern Ghana. *Journal of African Earth Sciences*, **153**, 208-218. https://www.sciencedirect.com/science/article/pii/S1464343X19300664 https://doi.org/10.1016/j.jafrearsci.2019.03.002

[10] Woguia, B.K., Nono, G.D.K., Tsoungui, P.E.N.E., Njiosseu, E.L.T., Kenne, P.A. and Nzenti, J.P. (2022) Geochemistry and U-Pb Zircon Age of the Paleoproterozoic Metasedimentary Rocks from the Bidou I, Nyong Series, Cameroon: Implications for Provenance and Tectonic Setting. *Arabian Journal of Geosciences*, **15**, Article No. 154. https://doi.org/10.1007/s12517-022-09476-7

[11] McLennan, S.M., Taylor, S.R., McCulloch, M.T. and Maynard, J.B. (1990) Geochemical and Nd Sr Isotopic Composition of Deep-Sea Turbidites: Crustal Evolution and Plate Tectonic Associations. *Geochimica et Cosmochimica Acta*, **54**, 2015-2050. https://www.sciencedirect.com/science/article/pii/001670379090269Q https://doi.org/10.1016/0016-7037(90)90269-Q

[12] Taylor, S.R. and McLennan, S.M. (1985) The Continental Crust: Its Composition and Evolution. https://www.osti.gov/biblio/6582885

[13] McDaniel, D.K., Hemming, S.R., McLennan, S.M. and Hanson, G.N. (1994) Resetting of Neodymium Isotopes and Redistribution of REEs during Sedimentary Processes: The Early Proterozoic Chelmsford Formation, Sudbury Basin, Ontario, Canada. *Geochimica et Cosmochimica Acta*, **58**, 931-941. https://www.sciencedirect.com/science/article/pii/0016703794905169 https://doi.org/10.1016/0016-7037(94)90516-9

[14] Ganne, J., Gerbault, M. and Block, S. (2014) Thermo-Mechanical Modeling of Lower Crust Exhumation—Constraints from the Metamorphic Record of the Palaeoproterozoic Eburnean Orogeny, West African Craton. *Precambrian Research*, **243**, 88-109. https://www.sciencedirect.com/science/article/pii/S0301926813003859 https://doi.org/10.1016/j.precamres.2013.12.016

[15] Bardet, M. (1974) Geologie du diamant II. Gisements de diamant d'Afrique.

[16] Pettijohn, F.J. (1972) The Archean of the Canadian Shield: A Resume. In: Doe, B.R. and Smith, D.K., Eds., *Studies in Mineralogy and Precambrian Geology*, Vol. 135, Geological Society of America, Boulder, 131-150.

https://pubs.geoscienceworld.org/gsa/books/book/140/chapter-abstract/3790066/The-Archean-of-the-Canadian-Shield-A-Resume?redirectedFrom=PDF
https://doi.org/10.1130/MEM135-p131

[17] Herron, M.M. (1988) Geochemical Classification of Terrigenous Sands and Shales from Core or Log Data. *Journal of Sedimentary Research*, **58**, 820-829. https://pubs.geoscienceworld.org/sepm/jsedres/article/58/5/820/98094/Geochemical-classification-of-terrigenous-sands
https://doi.org/10.1306/212F8E77-2B24-11D7-8648000102C1865D

[18] Roser, B.P. and Korsch, R.J. (1986) Determination of Tectonic Setting of Sandstone-Mudstone Suites Using SiO_2 Content and K_2O/Na_2O Ratio. *The Journal of Geology*, **94**, 635-650. https://doi.org/10.1086/629071

[19] Chapell, B.W. and White, A.J.R. (1974) Two Contrasting Types of Granites. *Pacific Geology*, **8**, 113-114.

[20] McLennan, S.M. (2001) Relationships between the Trace Element Composition of Sedimentary Rocks and Upper Continental Crust. *Geochemistry, Geophysics, Geosystems*, **2**, 2000GC000109. https://doi.org/10.1029/2000GC000109

[21] Rudnick, R. and Gao, S. (2003) Composition of the Continental Crust. In: Holland, H.D. and Turekian, K.K., Eds., *Treatise on Geochemistry*, Vol. 3, Elsevier, Amsterdam, 1-64. https://doi.org/10.1016/B0-08-043751-6/03016-4

[22] McLennan, S.M., Hemming, S., McDaniel, D.K. and Hanson, G.N. (1993) Geochemical Approaches to Sedimentation, Provenance, and Tectonics. Special Papers, Geological Society of America, Boulder, 21. https://books.google.ci/books?hl=fr&lr=&id=aUQCAQAAQBAJ&oi=fnd&pg=PA21&dq=%5B26%5D%09McLennan,+S.+M.,+Hemming,+S.,+McDaniel,+D.+K.,+%26+Hanson,+G.+N.+(1993).+Geochemical+approaches+to+sedimentation,+provenance,+and+tec-tonics.&ots=STIPs7y1Wt&sig=27RFaekhONW2-s_HGgrkx8CeTls&redir_esc=y#v=onepage&q&f=false
https://doi.org/10.1130/SPE284-p21

[23] Nesbitt, H.W., Markovics, G. and Price, R.C. (1980) Chemical Processes Affecting Alkalis and Alkaline Earth during Continental Weathering. *Geochimica et Cosmochimica Acta*, **44**, 1659-1666. https://www.sciencedirect.com/science/article/pii/0016703780902185
https://doi.org/10.1016/0016-7037(80)90218-5

[24] Nesbitt, H. and Young, G.M. (1982) Early Proterozoic Climates and Plate Motions Inferred from Major Element Chemistry of Lutites. *Nature*, **299**, 715-717. https://www.nature.com/articles/299715a0
https://doi.org/10.1038/299715a0

[25] Fedo, C.M., Wayne Nesbitt, H. and Young, G.M. (1995) Unraveling the Effects of Potassium Metasomatism in Sedimentary Rocks and Paleosols, with Implications for Paleoweathering Conditions and Provenance. *Geology*, **23**, 921-924. https://doi.org/10.1130/0091-7613(1995)023<0921:UTEOPM>2.3.CO;2

[26] Cox, R., Lowe, D.R. and Cullers, R.L. (1995) The Influence of Sediment Recycling and Basement Composition on Evolution of Mudrock Chemistry in the Southwestern United States. *Geochimica et Cosmochimica Acta*, **59**, 2919-2940. https://www.sciencedirect.com/science/article/pii/0016703795001859
https://doi.org/10.1016/0016-7037(95)00185-9

[27] Camire, G.E., Lafleche, M.R. and Ludden, J.N. (1993) Archaean Metasedimentary Rocks from the Northwestern Pontiac Subprovince of the Canadian Shield: Chemical Characterization, Weathering and Modelling of the Source Areas. *Precambrian Research*, **62**, 285-305. https://doi.org/10.1016/0301-9268(93)90026-X

https://www.sciencedirect.com/science/article/pii/030192689390026X

[28] Gao, S. and Wedepohl, K.H. (1995) The Negative Eu Anomaly in Archean Sedimentary Rocks: Implications for Decomposition, Age and Importance of Their Granitic Sources. *Earth and Planetary Science Letters*, **133**, 81-94. https://www.sciencedirect.com/science/article/pii/0012821X9500077P https://doi.org/10.1016/0012-821X(95)00077-P

[29] Joshi, K.B., Ray, S., Ahmad, T., Manavalan, S. and Aradhi, K.K. (2021) Geochemistry of Meta-Sediments from Neoproterozoic Shimla and Chail Groups of Outer Lesser Himalaya: Implications for Provenance, Tectonic Setting, and Paleo-Weathering Conditions. *Geological Journal*, **56**, 4451-4478. https://doi.org/10.1002/gj.4183

[30] Roser, B.P. and Korsch, R.J. (1985) Plate Tectonics and Geochemical Composition of Sandstones: A Discussion. *The Journal of Geology*, **93**, 81-84. https://doi.org/10.1086/628921

[31] McLennan, S.M. (1994) Rare Earth Element Geochemistry and the "Tetrad" Effect. *Geochimica et Cosmochimica Acta*, **58**, 2025-2033. https://www.sciencedirect.com/science/article/pii/0016703794902828 https://doi.org/10.1016/0016-7037(94)90282-8

[32] Hayashi, K.I., Fujisawa, H., Holland, H.D. and Ohmoto, H. (1997) Geochemistry of ~1.9 Ga Sedimentary Rocks from Northeastern Labrador, Canada. *Geochimica et Cosmochimica Acta*, **61**, 4115-4137. https://www.sciencedirect.com/science/article/pii/S0016703797002147 https://doi.org/10.1016/S0016-7037(97)00214-7

[33] Girty, G.H., Ridge, D.L., Knaack, C., Johnson, D. and Al-Riyami, R.K. (1996) Provenance and Depositional Setting of Paleozoic Chert and Argillite, Sierra Nevada, California. *Journal of Sedimentary Research*, **66**, 107-118. https://doi.org/10.1306/D42682CA-2B26-11D7-8648000102C1865D

[34] Nesbitt, H.W. and Young, G.M. (1984) Prediction of Some Weathering Trends of Plutonic and Volcanic Rocks Based on Thermodynamic and Kinetic Considerations. *Geochimica et Cosmochimica Acta*, **48**, 1523-1534. https://www.sciencedirect.com/science/article/pii/0016703784904083 https://doi.org/10.1016/0016-7037(84)90408-3

[35] Cullers, R.L., Bock, B. and Guidotti, C. (1997) Elemental Distributions and Neodymium Isotopic Compositions of Silurian Metasediments, Western Maine, USA: Redistribution of the Rare Earth Elements. *Geochimica et Cosmochimica Acta*, **61**, 1847-1861. https://www.sciencedirect.com/science/article/pii/S0016703797000483 https://doi.org/10.1016/S0016-7037(97)00048-3

[36] Shaw, D.M. (1968) A Review of K-Rb Fractionation Trends by Covariance Analysis. *Geochimica et Cosmochimica Acta*, **32**, 573-601. https://www.sciencedirect.com/science/article/pii/0016703768900501 https://doi.org/10.1016/0016-7037(68)90050-1

[37] Bhatia, M.R. (1983) Plate Tectonics and Geochemical Composition of Sandstones. *The Journal of Geology*, **91**, 611-627. https://doi.org/10.1086/628815

[38] Bhatia, M.R. (1985) Rare Earth Element Geochemistry of Australian Paleozoic Graywackes and Mudrocks: Provenance and Tectonic Control. *Sedimentary Geology*, **45**, 97-113. https://doi.org/10.1016/0037-0738(85)90025-9 https://www.sciencedirect.com/science/article/pii/0037073885900259

[39] Bhatia, M.R. and Crook, K.A. (1986) Trace Element Characteristics of Graywackes and Tectonic Setting Discrimination of Sedimentary Basins. *Contributions to Mineralogy and Petrology*, **92**, 181-193. https://doi.org/10.1007/BF00375292

[40] Chen, B. and Jahn, B.M. (2002) Geochemical and Isotopic Studies of the Sedimentary and Granitic Rocks of the Altai Orogen of Northwest China and Their Tectonic Implications. *Geological Magazine*, **139**, 1-13. https://doi.org/10.1017/S0016756801006100

[41] Maynard, J.B., Valloni, R. and Yu, H.S. (1982) Composition of Modern Deep-Sea Sands from Arc-Related Basins. *Geological Society, London, Special Publications*, **10**, 551-561. https://doi.org/10.1144/GSL.SP.1982.010.01.36

[42] McLennan, S.M. and Taylor, S.R. (1991) Sedimentary Rocks and Crustal Evolution: Tectonic Setting and Secular Trends. *The Journal of Geology*, **99**, 1-21. https://doi.org/10.1086/629470

[43] Koffi, A.Y., Kouamelan, A.N., Djro, S.C., Hervé, K.F.J.L., Raoul, T.K., Roland, K.B. and Stéphane, K.G.R. (2018) Pétrographie et origine des métasédiments du domaine SASCA (SW de la Côte d'Ivoire). *International Journal of Innovation and Applied Studies*, **23**, 451-464. https://www.proquest.com/openview/9df96268e640e1dc8d6695b4fcc9087f/1?pq-origsite=gscholar&cbl=2031961

[44] Koffi, A.M.P., Yacouba, C., Zié, O. and Inza, C. (2018) Caractéristiques petrographiques et géochimiques des métasédiments de la partie sud-est du bassin de la comoé (nord d'alépé-sud est de la côte d'ivoire). *Revue RAMReS*, **6**, 28-35. https://www.academia.edu/42413072/Science_de_la_vie_de_la_terre_et_agronomie